Hole transport in boron delta-doped diamond structures

Gauthier Chicot, Thu Nhi Tran Thi, Alexandre Fiori, François Jomard, Etienne Gheeraert, Etienne Bustarret, Julien Pernot

Hole transport in boron delta-doped diamond structures

G. Chicot,[1,a)] T. N. Tran Thi,[1] A. Fiori,[1] F. Jomard,[2] E. Gheeraert,[1] E. Bustarret,[1] and J. Pernot[1]
[1]*Institut Néel, CNRS and Université Joseph Fourier, BP166, 38042 Grenoble Cedex 9, France*
[2]*Groupe d'Étude de la Matière Condensée (GEMaC), UMR 8635 du CNRS, UVSQ, 45 Avenue des États-Unis, 78035 Versailles Cedex, France*

(Received 1 September 2012; accepted 1 October 2012; published online 15 October 2012)

The temperature dependence of the hole sheet density and mobility of four capped delta boron doped [100]-oriented epilayers has been investigated experimentally and theoretically over a large temperature range ($6\,K < T < 500\,K$). The influence of the parallel conduction through the thick buffer layer overgrown on the diamond substrate was shown not to be negligible near room temperature. This could lead to erroneous estimates of the hole mobility in the delta layer. None of the delta-layers studied showed any quantum confinement enhancement of the mobility, even the one which was thinner than 2 nm. © *2012 American Institute of Physics*.
[http://dx.doi.org/10.1063/1.4758994]

Due to outstanding physical properties (large carrier mobility, high breakdown voltage, and exceptional thermal conductivity), diamond is the ultimate semiconductor for high power and high frequency applications. These features should in principle allow to develop new low loss electric switches.[1] However, because of the high ionization energy of the boron *p*-type dopant,[2,3] the equilibrium carrier concentration is low at room temperature, and thus the on-state resistivity is very high. It has been proposed to overcome this problem by using boron δ-doping,[4,5] i.e., a highly doped layer (metallic $[B] \geq 5 \times 10^{20}\,cm^{-3}$) stacked between two intrinsic layers, resulting in a conduction combining a high mobility (due to a confinement-induced delocalisation of carriers away from the ionized impurities) with a large carrier concentration (due to metallic behavior). Recently, several groups reported fabrication and electrical measurements of such structures. Most of the electronic properties (sheet density and mobility) of the δ structures have been characterized by means of a field effect transistor (FET).[6,7] Temperature dependent impedance spectroscopy measurements have been recently performed to identify the different conduction paths in the stacked structures.[8,9] Hall effect combined to four probes resistivity measurements have also been used to measure the sheet density (p_S) and the carrier mobility (μ_H).[9,10] The most recent of these works reported a low sheet density ($p_S \simeq 10^{13}\,cm^{-2}$) and a hole mobility ($\mu_H = 13\,cm^{-2}/V \cdot s$) larger than the one expected for highly doped diamond at room temperature in δ-structures on [111]-oriented diamond substrates.[9] Unfortunately, no temperature dependence of p_S and μ_H in δ structures has been reported so far. It will be shown in this work that the analysis of the temperature dependence of $p_S(T)$ and $\mu_H(T)$ is essential in order to distinguish the contribution of each conduction path (buffer/high B-doped layer/cap layer) to the measured (mixed) conductivity. A correct analysis of the *apparent* Hall mobility and sheet density is expected to yield the real hole mobility in the δ-layer or at its interfaces.

The aim of this work was to investigate and describe the temperature dependence of the electrical transport properties of thin B-doped diamond embedded between non intentionally doped diamond layers in order to evaluate reliably the carrier mobility and density in the 2D hole gas. In the first part, a brief description of the samples fabrication and details about transport experiments will be given. In the second part, the temperature dependence of the hole sheet density and mobility will be described and analyzed. Finally, it will be shown that a δ-doped layer thinner than 2 nm has been grown and that no mobility enhancement, due to quantum confinement of the holes, was observed.

Four boron doped samples were grown by microwave plasma-enhanced chemical vapor deposition (MPCVD) on Ib-type [100]-oriented $3 \times 3\,mm^2$ diamond substrates (purchased from Sumitomo Electric) and consisting of a highly *p*-doped ($[B] \geq 5 \times 10^{20}\,cm^{-3}$) layer of thickness lower than 35 nm grown on a thick non intentionally doped (NiD) buffer layer suited for high mobility transport[3] and covered by another thin NiD cap layer (from 30 to 65 nm) with similar nominal properties. The buffer layer was grown in a $CH_4/O_2/H_2$ mixture (1%, 0.25%, 0.9875 molar) for 20 min (80 for sample #1). In the case of sample #1, the heavily doped layer was grown in a $CH_4/B_2H_6/H_2$ mixture (4%, 1500 ppm, 0.96 M), then etched *ex situ* in a H_2/O_2 plasma, and then a thin non intentionally cap layer was slowly overgrown. The heavily doped delta layer of the 3 other samples were grown in a more diluted $CH_4/B_2H_6/H_2$ mixture (0.5%, 6000 ppm, 0.995 M) before being etched in situ in H_2/O_2 and then covered by a thin cap layer grown in the same gas mixture as the initial buffer layer. Please note that in this second case the plasma was kept on throughout the whole process, as described elsewhere.[11] The role of the etching step is to reduce the highly *p*-doped layer thickness and to improve the B-doping profile sharpness at the top interface of the highly doped layer (reduce the residual doping in NiD due to memory effect of the reactor).

Hall bars have been fabricated on each sample in order to perform Hall effect and four probes resisitivity measurements. The bars were delineated by O_2 electron cyclotron

[a)]Electronic mail: gauthier.chicot@grenoble.cnrs.fr.

TABLE I. Summary of electrical transport characteristics of the four samples: Hall mobility and Hall sheet carrier density measured at 6 K and 300 K and thickness of cap layer/δ-layer/buffer layer (measured by SIMS unless specified otherwise).

Sample	Thickness (nm) cap/δ/buffer	p_S (cm^{-2}) (T = 6 K)	μ_H ($cm^2/V\,s$) (T = 6 K)	p_S (cm^{-2}) (T = 300 K)	μ_H ($cm^2/V\,s$) (T = 300 K)
#1	50/< 8[a]/900	4.0×10^{14}	1.3	1.4×10^{13}	54.6
#2	~30[b]/<2[a]/~300[b]	1.0×10^{14}	2.8	1.6×10^{14}	3.3
#3	40/35/290	4.2×10^{15}	3.1	4.4×10^{15}	2.9
#4	65/20/320	2.3×10^{15}	3.1	2.3×10^{15}	4.4

[a]Measured by Hall effect.
[b]Estimated from growth time.

resonance plasma etching of the diamond which surrounds the mesa. Ti/Pt/Au pads have been deposited and then annealed at 750 °C under vacuum (<10^{-8} mbar) during 30 min in order to obtain ohmic contact. Hall effect measurements were performed under well controlled conditions between 6 K and 500 K. Ohmicity of contacts was checked by $I(V)$ measurement over the whole range of temperature. Hall effect measurements were carried out with a dc magnetic field **B** (amplitude of 0.8 T) in the standard configuration (i.e., **B** parallel and j, the current density, perpendicular to the growth axis [100]).

The samples can be classified in two categories with two distinct behaviors (shown in Fig. 1 and summarized in Table I). On one hand, sample #1 shows a two-regime conduction: in the lowest temperature range (6 K < T < 150 K), a metallic conduction characterized by constant values of the mobility and the sheet carrier density, and then, above 150 K, an increase of the mobility and a decrease of the density versus temperature up to 350 K. On the other hand, samples #2, #3, and #4 exhibit a typical metallic conduction (finite conductivity at low temperature) with a constant carrier density and a low mobility ($1 < \mu_H < 4\,cm^2/V\,s$) over the whole temperature range.

The two conduction regimes of sample #1 can be described quantitatively using a multi layer Hall effect model recently detailed by Look.[12] The two-layer Hall effect model

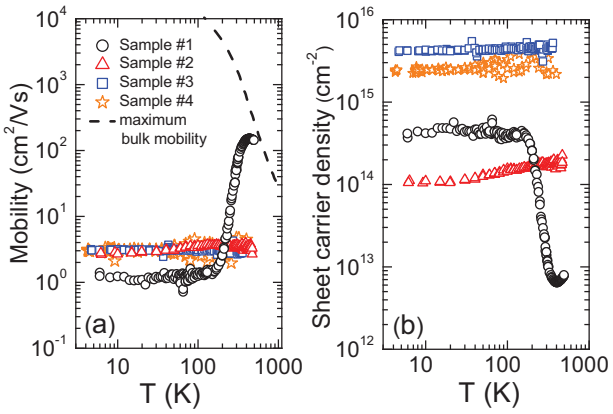

FIG. 1. (a) Hall mobility and (b) Hall sheet carrier density versus temperature of highly doped layers of different thicknesses (from less than 2 nm to 35 nm) grown on a thick non intentionally doped (NiD) buffer and covered by another thin NiD cap layer investigated using mesa-etched Hall bars. The symbols are experimental data and the dashed line is the calculated mobility for uncompensated diamond using the procedure and parameters described in Ref. 15.

with arbitrary surface dopant profiles[12] has been used here to investigate important characteristics of the δ-doped structure: (i) the influence of the sharpness of the boron acceptor profile and (ii) the influence of the buffer layer on the total hole conduction of the structure (conductivity, mobility, and sheet density). The transition between the maximum of B-doped (δ-layer) and the buffer could provide a second conduction channel in the valence band. In order to quantify this contribution, the carrier density along the whole profile was calculated using the neutrality equation in the case of Fermi Dirac statistics,[13] including the boron ionization energy doping dependence of Ref. 14 and the parameters detailed in Ref. 15. The compensation has been considered negligible in a first approximation, and the B-profile was taken as the only input parameter. The mobility associated to each B-doping level has been evaluated using the empirical procedure detailed in Ref. 3. Typically, for a 2 nm thick δ-layer (thickness of the sheet with a doping level $[B] = 5 \times 10^{20}\,cm^{-3}$) and a $[B]$ profile decreasing within 1 nm by one doping concentration decade from the δ-layer to the buffer and top layers, a sheet density (mobility) decrease (increase) of less than 40% (5%) was evaluated in comparison with the case of an abrupt profile. For a smooth transition within 10 nm by doping concentration decade, the sheet carrier density (mobility) at 500 K would be 2.5 times lower (2.5 higher) than the one expected in the case of an abrupt profile. These orders of magnitude are far from the variations observed in sample #1. Finally, the second possibility investigated here is the hole conduction through the buffer layer. Indeed, using the B concentration measured by secondary ion mass spectroscopy SIMS (see Fig. 2, $[B] = 3 \times 10^{16}\,cm^{-3}$), assuming a typical compensation[3] of $10^{15}\,cm^{-3}$, homogeneously distributed throughout the 850 nm of the buffer layer (this active

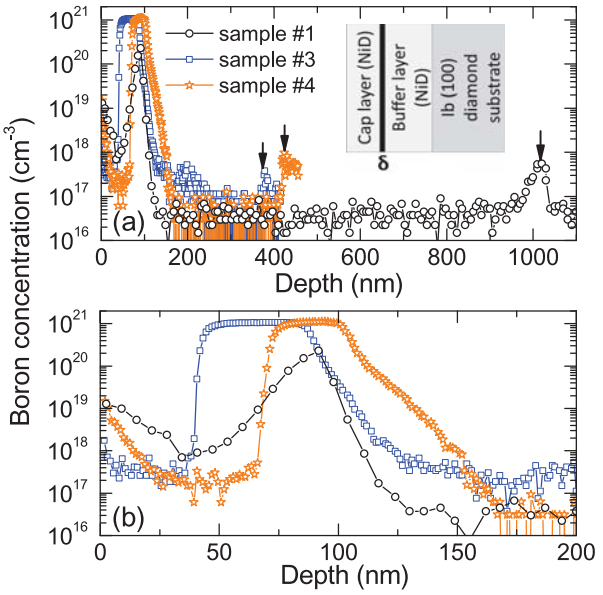

FIG. 2. (a) Secondary ion mass spectroscopy (SIMS) analysis of samples #1, #3, and #4 with schematic of the layers stack in the insert and (b) a zoom on δ-layer part of SIMS analysis. The arrows on (a) mark the interface between buffer layer and substrate. On one hand, it is not relevant to determine maximum doping and doping gradient of sample #1 since SIMS analysis are not sufficiently sampled for this sample. On the other hand, doping transition width can be determined for samples #3 and #4 and are, respectively, 4 nm/dec and 3 nm/dec on top side and 13 nm/dec and 16 nm/dec on back side.

thickness takes into account the 200 insulating nm related to the extension of the space charge region in the B-doped layer resulting from the nitrogen *n*-type doping of the Ib-type substrate), we calculate the mobility, the sheet density, and the conductivity temperature dependence of the buffer layer (dashed lines in Fig. 3). Then, using a T-independent mobility and sheet carrier concentration for the metallic δ-doped region (dotted lines in Fig. 3, $\mu_H = 1.3\,\mathrm{cm^2/V\,s}$ and $p_S = 4 \times 10^{14}\,\mathrm{cm^{-2}}$), we calculated the mixed mobility and sheet density corresponding to the abrupt junction between these two layers (full lines in Fig. 3). The resulting simulated mobility and sheet carrier density are plotted in Fig. 3.

As shown in Fig. 3, calculated values are in agreement with the experimental data. The observed temperature dependences were induced by a mixed conduction in both a thin metallic (highly *p*-doped) layer and the buffer and top (NiD) layers allowing higher mobilities. At low temperatures, the metallic layer (δ layer) controls completely the apparent mobility and sheet density, but while the temperature increased, the dopants of the thick buffer ($0.85\,\mu$m) become ionized and the buffer layer contributes to the total conduction of the structure. The δ-layer cannot be considered alone to describe the experimental data of the structure in the high temperature range $T > 150\,K$. The carriers responsible of the conduction at high temperature come from the B-dopant in the buffer and are not due to a delocalisation of the carrier from the δ-layer. The apparent mobility became closer to the high mobility of the buffer layer at higher temperatures (see Fig. 3(a)), when the sheet carrier density p_S decreases (see Fig. 3(b)) to that of the lightly doped layer (lower that of the δ-layer). Since the rise of the mobility is counterbalanced by the decrease in p_S, the sheet conductivity does not show a strong variation over the measured temperature range (not shown). In conclusion, the mobility and sheet density measured by Hall effect at room temperature are not relevant to the δ-layer in the case of a thick buffer layer. A temperature dependent measurement is needed in order to identify the contribution of each layer of the δ-doped structure to the total conduction and so to the apparent mobility.

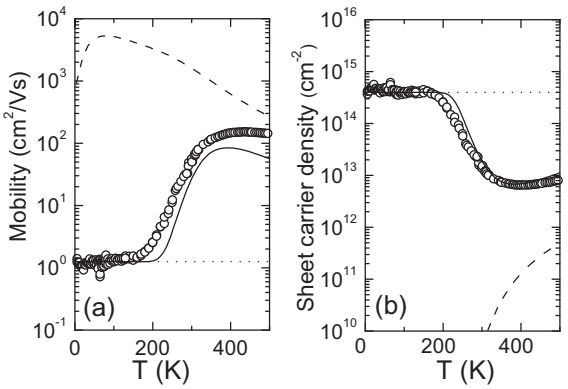

FIG. 3. (a) Hall mobility and (b) Hall sheet carrier density versus temperature of sample #1. The dashed lines correspond to the calculated values in the buffer layer with $[B] = 3 \times 10^{16}\,\mathrm{cm^{-3}}$ (SIMS) and compensation equals to $10^{15}\,\mathrm{cm^{-3}}$ distributed over the 850 nm active layer. The dotted lines are the values assumed for the metallic highly doped region (T-independent and values measured at 5 K, $\mu_H = 1.3\,\mathrm{cm^2/V\,s}$ and $p_S = 4 \times 10^{14}\,\mathrm{cm^{-2}}$). The full lines correspond to the two layers Hall mobility and sheet density using a multilayer Hall effect model.

A way to avoid this problem is to grow a sufficiently thin buffer layer (active layer thinner than 100 nm for a 2 nm thick δ-doped layer). This is the case of the three samples studied in the following part.

For samples #2, #3, and #4, the constant sheet carrier density and mobility measured over the whole range of temperature are typical of metallic conduction. When the metal-insulator transition (MIT)[16] is reached, the Fermi level is no longer in the forbidden gap but in the valence band, meaning that all the dopants are ionized over the whole temperature range. For sample #3, SIMS analysis (cf., Fig. 2) yields a thickness of 35 nm and a maximum doping level of $[B] = 1 \times 10^{21}\,\mathrm{cm^{-3}}$ and 20 nm at $[B] = 1 \times 10^{21}$ for sample #4, while no SIMS analysis was undertaken on sample #2 because of its expected very low thickness. In fact, as it has been shown[17] particularly in the case of ultra thin highly doped layers, SIMS analysis is not free of artifacts[18] because of ion mixing doping transition width at NiD/δ interfaces is overestimated, resulting in erroneous values of δ thickness or maximum doping level value.

In order to evaluate reliably the highly *p*-doped layer thickness, iso-lines corresponding to the measured value of sheet carrier density (iso-p_s) are plotted in a graph showing boron concentration versus thickness of the highly *p*-doped layer (cf., Fig. 4). For the metallic conduction observed in the samples under study (i.e., finite conductivity at low temperature), the boron concentration must be at least equal or larger than $5 \times 10^{20}\,\mathrm{cm^{-3}}$ (critical boron concentration for the MIT[16]). Also, by plotting the sheet carrier density measured experimentally in a metallic sample, the maximum thickness of the δ-doped layer can be directly read out at the intercept with the horizontal line corresponding to the critical concentration of the MIT transition. The isolines of the four samples of this work are plotted in Fig. 4. This method is not useful for samples #3 and #4, since the highly doped layer of these samples are thick enough (more than 20 nm) to be

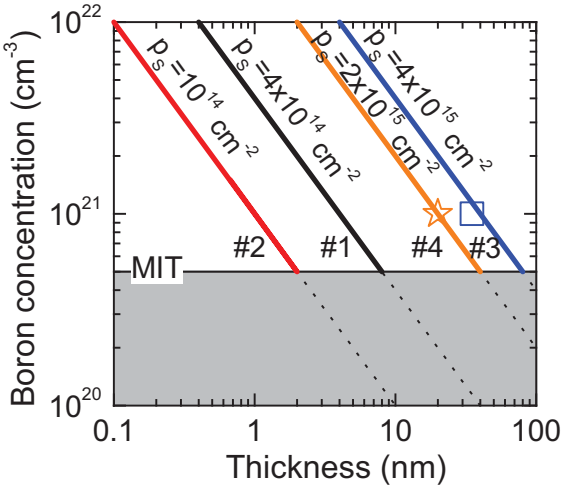

FIG. 4. Iso-sheet carrier density lines measured by Hall effect plotted on a boron concentration ($\mathrm{cm^{-3}}$) versus thickness (nm) map. For $[B] \geq 5 \times 10^{20}\,\mathrm{cm^{-3}}$, the conduction is metallic. The intercepts of the lines (boundaries between full and dashed) with the horizontal line corresponding to the critical concentration for the MIT give the maximum thickness of the highly doped region where $[B] > 5 \times 10^{20}\,\mathrm{cm^{-3}}$. The symbols are SIMS data for sample #3 (square) and sample #4 (star).

measured accurately by SIMS. The SIMS data (B-doping and thickness of the δ-layer) are reported in Fig. 4 (open square for sample #3 and open star for sample #4), in good agreement with the Hall data ($p_S = 4 \times 10^{15}\,\mathrm{cm}^{-2}$ for sample #3 (blue line) and $p_S = 2 \times 10^{15}\,\mathrm{cm}^{-2}$ for sample #4 (orange line)) showing a full activation of B-dopants. For sample #1 (black line), the iso-$p_s = 4 \times 10^{14}\,\mathrm{cm}^{-2}$ (value of sheet carrier density at low temperature) indicates that the thickness of the highly doped layer is less than 8 nm. By doing the same way with iso-$p_s = 10^{14}\,\mathrm{cm}^{-2}$ of sample #2 (red line), the highly p-doped layer is found to be equal or thinner than 2 nm. Calculations based only on the hole distribution in the V-shape potential suggest that delocalisation would occur for δ under 3 nm.[19] The highly p-doped layer of sample #2 is rather thin, but the mobility measured is around $3\,\mathrm{cm}^2/\mathrm{Vs}$, which is typically the same than the one measured in thicker highly p-doped layer like sample #3 (cf., Fig. 1). The result shows that the strong coulombic scattering induced by ionized boron atoms and screened by the free holes (Fermi screening radius about 0.3 nm) in the δ-layer limits the mobility of the free hole in the same way than in a bulk material. No quantum confinement enhancement of the mobility is observed for a δ with $p_s = 10^{14}\,\mathrm{cm}^{-2}$ corresponding to a maximum thickness of 2 nm, suggesting that thinner δ-layers or/and with sharper interfaces should be grown (i.e., $p_s < 10^{14}\,\mathrm{cm}^{-2}$).

To summarize, it has been shown that no quantum confinement enhancement of the mobility was present even for δ thickness of 2 nm using transport measurements to evaluate mobility, sheet carrier density, and thickness. Low temperature Hall effect is a useful tool to evaluate the doping/thickness window. This approach becomes necessary for very thin δ-layers for which SIMS data could be erroneous or when parallel conduction in a thick buffer layer leads to an apparent mobility enhancement at room temperature.

The authors would like to thank B. Fernandez (microfabrication) and P. Giroux (growth), Institut Néel, CNRS, for their technical support. Funding for this project was provided by grants from la Région Rhône-Alpes, and Agence Nationale de la Recherche under Grant No. ANR-08-0195.

[1]R. S. Balmer, I. Friel, S. Woollard, C. J. Wort, G. Scarsbrook, S. Coe, H. El-Hajj, A. Kaiser, A. Denisenko, E. Kohn, and J. Isberg, Philos. Trans. R. Soc. A **366**, 251 (2008).
[2]J. P. Lagrange, A. Deneuville, and E. Gheeraert, Diamond Relat. Mater. **7**, 1390 (1998).
[3]P.-N. Volpe, J. Pernot, P. Muret, and F. Omnès, Appl. Phys. Lett. **94**, 092102 (2009).
[4]T. Kobayashi, T. Ariki, M. Iwabuchi, T. Maki, S. Shikama, and S. Suzuki, J. Appl. Phys. **76**, 1977 (1994).
[5]E. F. Schubert, *Delta-Doping of Semiconductors* (Cambridge University Press, 1996).
[6]H. El-Hajj, A. Denisenko, A. Kaiser, R. S. Balmer, and E. Kohn, Diamond Relat. Mater. **17**, 1259 (2008).
[7]A. Aleksov, A. Vescan, M. Kunze, P. Gluche, W. Ebert, E. Kohn, A. Bergmeier, and G. Dollinger, Diamond Relat. Mater. **8**, 941 (1999).
[8]N. Tumilty, J. Welch, H. Ye, R. S. Balmer, C. Wort, R. Lang, and R. B. Jackman, Appl. Phys. Lett. **94**, 052107 (2009).
[9]R. Edgington, S. Sato, Y. Ishiyama, R. Morris, R. B. Jackman, and H. Kawarada, J. Appl. Phys. **111**, 033710 (2012).
[10]M. Kunze, A. Vescan, G. Dollinger, A. Bergmaier, and E. Kohn, Carbon **37**, 787 (1999).
[11]A. Fiori, T. N. Tran Thi, G. Chicot, F. Jomard, F. Omnès, E. Gheeraert, and E. Bustarret, Diamond Relat. Mater. **24**, 175 (2012).
[12]D. C. Look, J. Appl. Phys. **104**, 063718 (2008).
[13]J. Pernot, W. Zawadzki, S. Contreras, J. L. Robert, E. Neyret, and L. Di Cioccio, J. Appl. Phys. **90**, 1869 (2001).
[14]J. P. Lagrange, A. Deneuville, and E. Gheeraert, Carbon **37**, 807 (1999).
[15]J. Pernot, P. N. Volpe, F. Omnès, P. Muret, V. Mortet, K. Haenen, and T. Teraji, Phys. Rev. B **81**, 205203 (2010).
[16]T. Klein, P. Achatz, J. Kacmarcik, C. Marcenat, F. Gustafsson, J. Marcus, E. Bustarret, J. Pernot, F. Omnès, B. E. Sernelius, C. Persson, A. F. da Silva, and C. Cytermann, Phys. Rev. B **75**, 165313 (2007).
[17]A. Takano, Y. Homma, Y. Higashi, H. Takenaka, S. Hayashi, K. Goto, M. Inoue, and R. Shimizu, Appl. Surf. Sci. **203**, 294 (2003).
[18]S. Hofmann, Surf. Interface Anal. **30**, 228 (2000).
[19]A. Fiori, J. Pernot, E. Gheeraert, and E. Bustarret, Phys. Status Solidi A **207**, 2084 (2010).